

Ubiquitin-like Protein Domains Show High Resistance to Mechanical Unfolding Similar to That of the I27 Domain in Titin: Evidence from Simulations

Pai-Chi Li and Dmitrii E. Makarov*

Department of Chemistry and Biochemistry and Institute for Theoretical Chemistry, University of Texas at Austin, Austin, Texas 78712

Received: August 11, 2003; In Final Form: October 27, 2003

The I27 domain in the muscle protein titin can sustain large mechanical forces without unfolding. Recently it has been suggested [Eom, K.; Li, P.-C.; Makarov, D. E.; Rodin, G. J. *J. Phys. Chem. B* 2003, 107, 8730] that the “clamp” formed by the parallel strands in this domain represents an optimal topology maximizing the mechanical strength of cross-linked polymer chains. Here we use simulations to demonstrate that protein G IgG-binding domain III and ubiquitin, both exhibiting a parallel strand arrangement similar to that in I27 but otherwise having a distinctly different fold and not involved in an obvious load-bearing function, exhibit high resistance to mechanical unfolding. Using molecular dynamics simulations, we compute the potential of mean force as a function of the distance between the domains’ C- and N-termini and use transition state theory to calculate the force-dependent rates of unfolding. We further predict the outcome of a hypothetical single-molecule AFM pulling experiment, in which one of the I27 domains in titin is replaced by one of the above two proteins. For typical AFM pulling rates, the predicted unfolding force is in the range 190–220 pN for ubiquitin and 100–150 pN for the IgG-binding domain.

1. Introduction

Single molecule pulling experiments, in which proteins are unfolded by mechanical forces, provide a wealth of information about the mechanical properties of proteins that have load-bearing functions in living organisms.^{1–29} Certain proteins, such as titin, can sustain large forces and dissipate large amounts of energy in the course of their mechanical unfolding.^{14,19,20,22,30,31} This dissipated energy is often considerably larger than the free energy of folding.³² This property is believed to account for the remarkable toughness of many natural materials.²² On the other hand, nonmechanical proteins such as barnase often exhibit very little resistance to mechanical unfolding.⁴

Naturally occurring load-bearing proteins often contain sequences of tandemly repeated domains. It is possible to incorporate domains that are not commonly found in natural mechanical proteins into genetically engineered “polyprotein” chains.^{3,4,33} Such chains may have novel mechanical properties and have potential applications in fiber and tissue engineering. The overall mechanical response of natural or engineered polyproteins is controlled by the mechanical properties of the constituent individual domains.

Recently we have studied³⁴ the relationship between the topology and the mechanical unfolding mechanisms of cross-linked polymer chains. Viewing those as caricatures of proteins, we discovered that the maximum resistance to unfolding (measured either as the peak force or as the energy dissipated in the course of unfolding) is achieved if the cross-links are organized into a “clamp” formed by parallel strands. It had been previously noticed that the high mechanical strength of the immunoglobulin-like domain I27 of titin is related to the presence of such a clamp in the domain,^{5,14,30,31} suggesting that its optimality may indeed be utilized in some structural proteins. One may then wonder whether other protein domains, not necessarily having any mechanical function and exhibiting folds

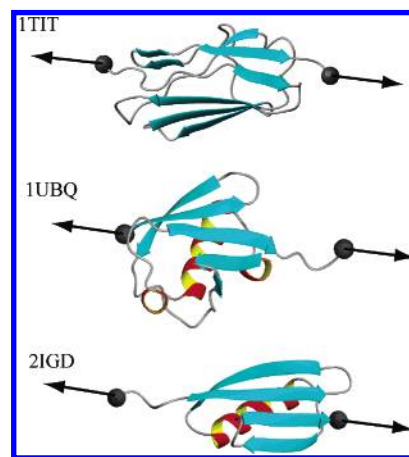


Figure 1. Structures of I27, ubiquitin, and protein G domains (pdb codes 1TIT, 1UBQ, and 2IGD, respectively). Arrows indicate at which points the force was applied in the simulation. This figure was generated with MOLMOL software.⁵⁸

different from the β -sandwich fold of I27 but having a similar parallel strand arrangement, would also be highly mechanically resistant.

In this paper we present evidence that this is indeed the case. We study the mechanical unfolding of two mixed $\alpha + \beta$ domains, streptococcal protein G IgG-binding domain III (Protein Databank (pdb) code 2IGD) and ubiquitin (pdb code 1UBQ), both having a β -grasp fold, and show that they display high resistance to unfolding similar to that of I27 and that, as in the case of I27, their mechanical unfolding mechanisms involve separation of parallel strands. See Figure 1 for the structures of these two domains along with the I27 domain. We further predict the outcome of an AFM pulling experiment, in which an I27 domain is replaced by one of the above two domains. One of the two proteins, ubiquitin, has recently been

studied experimentally,³⁵ and the unfolding forces found in our simulation are close to those measured experimentally. To our knowledge, the second protein has not been studied experimentally so far.

2. Methods

A force f applied at the ends of a protein domain may cause it to unfold. If f is not too high, then the domain unfolding is a thermally activated barrier crossing process that can be described by a force-dependent unfolding rate constant $k_u(f)$ (assuming that unfolding is a first-order process, which was found to be the case, e.g., for the I27 domain in titin¹⁹). To calculate $k_u(f)$, one can use transition state theory. We describe the state of the domain by using a single reaction coordinate, the domain extension R , defined as the distance between its first and last α -carbon atoms. The rate constant $k_u(f)$ can be calculated if the free energy of the domain $G(R)$ is known as a function of R . Further, the validity of the assumption that unfolding is a two-state process characterized by a single rate constant is related to the shape of $G(R)$: multiple minima in $G(R)$ would be indicative of unfolding intermediates.

To compute $G(R)$, we used the procedure described in our earlier paper.³⁶ Here we give a brief summary of our method:

For a set of values $R_0 = R_0(i)$, $i = 1, 2, \dots, M$, spanning the range of extensions of interest, we perform molecular dynamics (MD) simulations of the domain with a penalty term^{4,30,31,37,38}

$$V(R, R_0) = k_c(R - R_0)^2/2 \quad (1)$$

added to its energy. The force constant k_c used in the calculations was equal to 1.38 N/m. The penalty term introduces a bias that ensures that the MD simulation efficiently samples extensions R in the vicinity of R_0 . For each value of the distance restraint R_0 , we compute the equilibrium distribution of the extension R , which is related to the potential of mean force $G(R)$ according to the equation

$$p_{R_0}(R) \propto \exp[-(G(R) + k_c(R - R_0)^2/2)/k_B T] \quad (2)$$

allowing accurate reconstruction of $G(R)$ in the vicinity of R_0 :

$$G(R) = -k_B T \ln p_{R_0}(R) - (1/2)k_c(R - R_0)^2 + \text{constant} \quad (3)$$

The optimum estimate for $G(R)$ is obtained by using the self-consistent histogram method,^{39,40} in which it is constructed as a linear combination of the estimates obtained for each value of R_0 :

$$\exp(-G_{\text{opt}}(R)/k_B T) = \sum_i w_i(R) z_i \exp(-G_i(R)/k_B T) \quad (4)$$

where $\sum_i w_i(R) = 1$ and $G_i(R)$ is the estimate for $G(R)$ obtained from eq 3 with $R_0 = R_0(i)$. The normalization factors z_i and the weights $w_i(R)$ are obtained by minimizing the error, leading to self-consistent equations

$$\begin{aligned} \exp[-G_{\text{opt}}(R)/k_B T] = & \sum_i p_{R_0(i)}(R) / \sum_i z_i^{-1} \exp[-(1/2)k_c(R - R_0(i))^2/k_B T] \\ z_n = \int dR \exp[-(1/2)k_c(R - R_0(n))^2/k_B T] & \sum_i p_{R_0(i)}(R) / \\ & \sum_i z_i^{-1} \exp[-(1/2)k_c(R - R_0(i))^2/k_B T] \end{aligned} \quad (5)$$

which are solved iteratively.

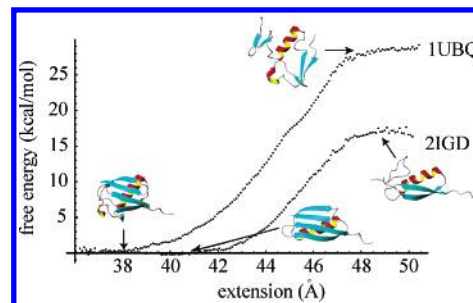


Figure 2. Potential of mean force $G(R)$ for 1UBQ and 2IGD. Representative structures corresponding to the folded state and to the unfolding transition state are also shown. The protein pictures were generated with the MOLMOL program.⁵⁸

The initial structures for the MD runs for different R_0 's were generated by using adiabatic mapping.^{41,42} We have started with the X-ray structure of the molecule and minimized its energy. Then we added the penalty term (1) to the energy. Starting with R_0 corresponding to the extension of the minimum energy structure, R_0 was increased in small ($\Delta R = 0.1$ Å) increments and the energy of the structure was reminimized in each step. This yielded locally minimal energy structures for each value $R_0(i)$, which were used to start each MD run. This method helps avoid potential problems caused by starting each simulation too far from the mechanical equilibrium. With this choice of initial conditions, the structures were found to equilibrate in a few picoseconds in each MD run. For each R_0 , we have run 50 ps of MD simulation at 298 K, with a time step of 1 fs. Both adiabatic mapping and MD simulations were performed with Tinker software (<http://dasher.wustl.edu/tinker/>) using the GB/SA solvation model⁴³ and the CHARMM27 force field.⁴⁴

3. Results

The potential of mean force $G(R)$ reconstructed from MD trajectories as described in section 2 is shown in Figure 2 for protein G IgG-binding domain III (2IGD) and ubiquitin (1UBQ). In each case, after an initial rise, $G(R)$ levels out so that the corresponding equilibrium force $f_{\text{eq}} = G'(R)$ drops. This feature indicates that the domain no longer resists force and thus unfolds. Examination of the molecules' snapshots corresponding to the onset of this flat section of the $G(R)$ plot (Figure 2) shows that in each case the two parallel strands become separated. This unfolding scenario has previously been observed in the mechanical unfolding of the I27 domain of titin.^{14,30,31,36} The unfolding free energy barrier corresponding to the maximum of $G(R)$ is ≈ 29 kcal/mol for 1UBQ and ≈ 17 kcal/mol for 2IGD. For comparison, the unfolding barrier for the I27 domain was estimated to be ≈ 22 kcal/mol from both experimental data⁴⁵ and simulation.³⁶

In a typical AFM pulling experiment, the stretching force f applied between the ends of the molecule varies slowly compared to the time scale of molecular motions. For each f the domain then sees a (nearly) static potential $G_f(R)$ given by

$$G_f(R) = G(R) - fR \quad (6)$$

This potential is shown in Figure 3 for each protein for different values of the force f . As seen in Figure 3, application of a force lowers the unfolding barrier, which is defined as the difference between the maximum and the minimum values of the free energy $G_f(R)$.

$$\Delta G_u(f) = \max[G_f(R)] - \min[G_f(R)] \quad (7)$$

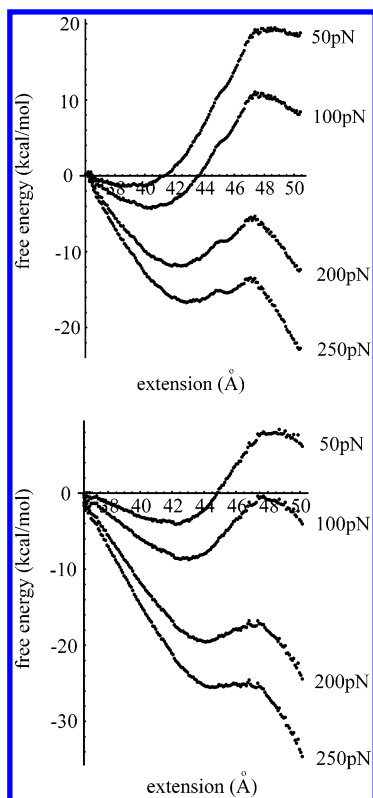


Figure 3. Unfolding free energy profile, eq 6, for (A) 1UBQ and (B) 2IGD for different values of the applied force: 50, 100, 200, and 250 pN.

Once the force is large enough, the free energy barrier disappears and the protein unfolds. For example, the barrier for 2IGD disappears when the applied force is ~ 250 pN. However, under typical experimental conditions domains unfold at forces that are lower than those required to completely wipe out the barrier $\Delta G_u(f)$ because it can be surmounted via activated barrier crossing.

The force-dependent rate of barrier crossing is given by transition state theory:

$$k_u(f) = \nu(f) \exp[-\Delta G_u(f)/k_B T] \quad (8)$$

If one assumes^{46–48} that the dynamics along the reaction coordinate $R(t)$ can be viewed as one-dimensional diffusive motion in the effective potential $G_f(R)$ obeying a Langevin equation,^{46–48} then the unfolding prefactor $\nu(f)$ can be estimated from Kramers' theory.⁴⁹ In the absence of memory effects and in the overdamped limit it is given by⁴⁹ $\nu(f) = (2\pi\eta)^{-1} \sqrt{G''(R_N(f))G''(R_{TS}(f))}$, where η is the friction coefficient and $R_N(f)$ and $R_{TS}(f)$ are the positions of the “native” well and the transition state (i.e., the minimum and the maximum of $G_f(R)$). A number of methods have been proposed to extract the friction coefficient from MD simulations;^{36,46–48} however, because the present simulation uses an implicit solvation model it cannot provide a first principles estimate for η . Here we simply chose the unfolding prefactor ν to be the same as that estimated for the I27 domain in our earlier study,³⁶ $\nu = 10^8 \text{ s}^{-1}$. Figure 4 illustrates how the unfolding rate constant depends on the force for each protein.

The mechanical unfolding of ubiquitin has been studied in single molecule pulling AFM experiments.³⁵ To our knowledge, there are no experimental data on the mechanical unfolding of 2IGD. As previously shown,^{19,36,50} one can use the computed unfolding rates $k_u(f)$ to predict the outcome of such AFM

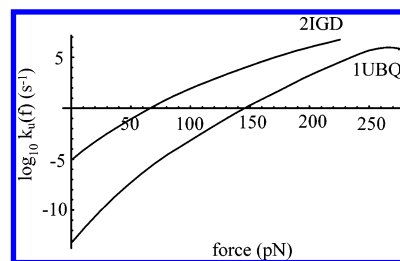


Figure 4. Unfolding rate constant as a function of applied force.

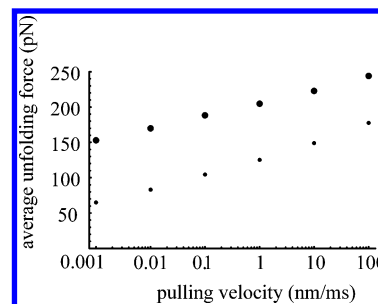


Figure 5. Predicted average unfolding force as a function of pulling speed for 1UBQ (●) and 2IGD (○).

experiments. Imagine a hypothetical experiment, in which one of the I27 domains in the titin molecule is replaced by either 2IGD or 1UBQ. If the molecule is stretched at a constant velocity u , the probability $p(t) dt$ that the domain unfolds between time t and $t + dt$ is given by

$$p(t) dt = k_u(f(t)) \exp[-\int_0^t k_u(f(t)) dt] dt \quad (9)$$

and the probability distribution for the unfolding force F is found from eq 9:

$$p(F) dF = \frac{p(t)}{|df(t)/dt|} \Big|_{f(t)=F} dF \quad (10)$$

In AFM experiments, one end of the chain is attached to a cantilever and the other end is fastened on a substrate that moves at a constant velocity u . To calculate the stretching force $f(t)$ as a function of time, one needs to know the compliance of the entire chain and the cantilever. If the cantilever is modeled as a harmonic spring with a force constant γ_c and the wormlike chain model^{51–53} is used to describe the overall compliance of the chain, then one finds^{19,36,50} $f(t)$ to be the solution of the equation

$$f(t) = \frac{k_B T}{l_p} \left[\frac{1}{4} \left(1 - \frac{(ut - f(t)/\gamma_c)}{L} \right)^{-2} - \frac{1}{4} + \frac{(ut - f(t)/\gamma_c)}{L} \right] \quad (11)$$

The persistence length $l_p = 4 \text{ Å}$, the contour length $L = 580 \text{ Å}$,^{19,20} and the cantilever force constant $\gamma_c = 0.06 \text{ N/m}$ ^{27,54} are chosen here to be the same as those in our previous study.³⁶ The predicted average unfolding force $\langle F \rangle = \int dF p(F)F$ is plotted as a function of the pulling speed u in Figure 5, showing that 2IGD would unfold at somewhat lower forces than ubiquitin and it would also exhibit a stronger dependence of $\langle F \rangle$ on the pulling rate. For typical AFM pulling speeds $u = 0.1–10 \text{ nm/ms}$ the unfolding force is in the range 100–150 pN for 2IGD and 190–220 pN for 1UBQ. For ubiquitin, the measured unfolding forces³⁵ are close to the values calculated here.

4. Concluding Remarks

The high mechanical resistance of ubiquitin-like domains appears to be accidental rather than necessitated by their

function. These $\alpha + \beta$ proteins display mechanical strength comparable to that of the β -sandwich domains implicated in load-bearing tasks in living organisms. Their mechanical unfolding mechanism is also similar to that of the I27 domain in the muscle protein titin and involves separation of two parallel strands, which are seen to be the key to their high resistance to unfolding.

It is interesting to compare the unfolding rates calculated here with those for thermal or chemical denaturation. For ubiquitin, we have calculated $k_u(0) = 5.5 \times 10^{-14} \text{ s}^{-1}$, 10 orders of magnitude smaller than the unfolding rate constant under native conditions, $k_{\text{chem}} \sim 4.3 \times 10^{-4} \text{ s}^{-1}$, which was extrapolated to zero denaturant concentration from ubiquitin chemical denaturing experiments.⁵⁵ We have seen a similar situation in our earlier study of the unfolding of the I27 domain in titin.³⁶ Linear extrapolation that assumes the unfolding barrier is a linear function of the force f and the unfolding rate constant obeys the equation

$$\ln k_u(f) = \ln k_u(0) - f\Delta x/k_B T \quad (12)$$

is routinely used for interpretation of the experimental data. [Note, however, the recent experimental evidence⁵⁶ that eq 12 breaks down in the case of the I27 domain for forces below 100 pN.] Equation 12 implies that the plots in Figure 4 are straight lines, an obviously incorrect assumption in our case. Because AFM probes a limited range of unfolding forces, eq 12 may be valid locally in this range. The value of $k_u(0)$ extrapolated from the experimental data by using eq 12 would then be higher than $k_u(0)$ calculated here.

A more intriguing question is why the calculated $k_u(0)$ is so much different from the intrinsic unfolding rate (which we identify with the chemical denaturation rate): in fact, the calculated mechanical unfolding rate $k_u(f)$ is lower than k_{chem} for $f < 90 \text{ pN}$. Given a good agreement of our simulations with experimental data in the experimental range of forces, it seems unlikely that simulation errors could account for such a large discrepancy. It is more likely that the reason is a poor choice of the unfolding coordinate. Our procedure here is essentially a variational transition state theory⁵⁷ calculation of the rate, in which a reaction coordinate measuring the unfolding progress is selected and the free energy barrier is computed along this coordinate. Imposing a large force between the C- and N-termini of the chain selects a natural unfolding coordinate equal to the extension R . However, R may be a poor reaction coordinate when the force f is small or zero. In a system that has a single transition state, a poor choice of the reaction coordinate can only lead to an overestimate for the rate constant because transition state theory ignores barrier recrossing. Thus one should expect that the true rate should be even smaller than estimated. However, if the system has multiple transition states, a poor choice of the reaction coordinate may lead to the sampling of the neighborhood of a "wrong" transition state (i.e., not the one with the lowest free energy barrier), since a 50 ps MD trajectory will be unlikely to ergodically sample the entire available conformational space. In other words, driven along the selected reaction coordinate, our system does not have enough time to "discover" the true (i.e., the lowest) unfolding transition state during the course of a short-time simulation. Thus the computed barrier will correspond to the wrong transition state and will be higher than the correct free energy barrier, resulting in an underestimate for the intrinsic unfolding rate. We thus expect that the unfolding pathway should change as the force is lowered and that the low-force unfolding pathway

cannot be probed by the present simulation because we do not have a good guess for the reaction coordinate in this case.

Acknowledgment. This work was supported by the Robert A. Welch Foundation and by the ACS Petroleum Research Fund. Discussions with Andres F. Oberhauser are gratefully acknowledged.

References and Notes

- (1) Lavery, R.; Lebrun, A.; Allemand, J.-F.; Bensimon, D.; Croquette, V. *J. Phys.: Condens. Matter* **2002**, *14*, R383–R414.
- (2) Becker, N.; Oroudjev, E.; Mutz, S.; Cleveland, J. P.; Hansma, P. K.; Hayashi, C. Y.; Makarov, D. E.; Hansma, H. G. *Nat. Mater.* **2003**, *2*, 278.
- (3) Best, R. B.; Brockwell, D. J.; Toca-Herrera, J. L.; Blake, A. W.; Smith, D. A.; Radford, S. E.; Clarke, J. *Anal. Chim. Acta* **2003**, *479*, 87–105.
- (4) Best, R. B.; Li, B.; Steward, A.; Daggett, V.; Clarke, J. *Biophys. J.* **2001**, *81*, 2344.
- (5) Brockwell, D. J.; Beddard, G. S.; Clarkson, J.; Zinober, R. C.; Blake, A.; Trinick, J.; Olmsted, P. D.; Smith, D. A.; Radford, S. E. *Biophys. J.* **2002**, *83*, 458.
- (6) Erickson, H. P. *Science* **1997**, *276*, 1090.
- (7) Fisher, T. E.; Marsalek, P. E.; Fernandez, J. M. *Nat. Struct. Biol.* **2000**, *7*, 719.
- (8) Fisher, T. E.; Oberhauser, A. F.; Vezquez, M. C.; Marsalek, P. E.; Fernandez, J. *TIBS* **1999**, *24*, 379.
- (9) Hansma, H. G.; Pietrasanta, L. *Curr. Opin. Chem. Biol.* **1998**, *2*, 579.
- (10) Hansma, H. G.; Pietrasanta, L. I.; Auerbach, I. D.; Sorenson, C.; Golan, R.; Holden, P. A. *J. Biomater. Sci., Polym. Ed.* **2000**, *11*, 675.
- (11) Kellermayer, M. S. Z.; Smith, S. B.; Granzier, H. L.; Bustamante, C. *Science* **1997**, *276*, 1112.
- (12) Li, H.; Carrion-Vazquez, M.; Oberhauser, A. F.; Marsalek, P. E.; Fernandez, J. M. *Nat. Struct. Biol.* **2000**, *7*, 1117.
- (13) Li, H.; Oberhauser, A. F.; Fowler, S. B.; Clarke, J.; Fernandez, J. M. *Proc. Natl. Acad. Sci. U.S.A.* **2000**, *97*, 6527.
- (14) Marsalek, P. E.; Lu, H.; Li, H.; Carrion-Vazquez, M.; Oberhauser, A. F.; Schulten, K.; Fernandez, J. *Nature* **1999**, *402*, 100.
- (15) Oberhauser, A. F.; Badilla-Fernandez, C.; Carrion-Vazquez, M.; Fernandez, J. M. *J. Mol. Biol.* **2002**, *319*, 433.
- (16) Oberhauser, A. F.; Hansma, P. K.; Carrion-Vazquez, M.; Fernandez, J. M. *Proc. Natl. Acad. Sci. U.S.A.* **2001**, *98*, 468–472.
- (17) Oberhauser, A. F.; Marsalek, P. E.; Erickson, H.; Fernandez, J. M. *Nature* **1998**, *393*, 181.
- (18) Pennisi, M. E. *Science* **1999**, *283*, 168.
- (19) Rief, M.; Fernandez, J. M.; Gaub, H. E. *Phys. Rev. Lett.* **1998**, *81*, 4764.
- (20) Rief, M.; Gautel, M.; Oesterhelt, F.; Fernandez, J. M.; Gaub, H. E. *Science* **1997**, *276*, 1109–1112.
- (21) Rief, M.; Pascual, J.; Saraste, M.; Gaub, H. E. *J. Mol. Biol.* **1999**, *286*, 553–561.
- (22) Smith, B. L.; Schaffer, T. E.; Viani, M.; Thompson, J. B.; Frederick, N. A.; Kindt, J.; Belcher, A.; Stucky, G. D.; Morse, D. E.; Hansma, P. K. *Nature* **1999**, *399*, 761.
- (23) Thompson, J. B.; Hansma, H. G.; Hansma, P. K.; Plaxco, K. W. *J. Mol. Biol.* **2002**, *322*, 645–652.
- (24) Thompson, J. B.; Kindt, J. H.; Drake, B.; Hansma, H. G.; Morse, D. E.; Hansma, P. K. *Nature* **2001**, *414*, 773.
- (25) Tskhovrebova, L.; Trinick, J. A.; Sleep, J. A.; Simmons, R. M. *Nature* **1997**, *387*, 308.
- (26) Viani, M. B.; Schaffer, T. E.; Chand, A.; Rief, M.; Gaub, H. E.; Hansma, P. K. *J. Appl. Phys.* **1999**, *86*, 2258–2262.
- (27) Viani, M. B.; Schaffer, T. E.; Paloczi, G. T.; Pietrasanta, I.; Smith, B. L.; Thompson, J. B.; Richter, M.; Rief, M.; Gaub, H. E.; Plaxco, K. W.; Cleland, A. N.; Hansma, H. G.; Hansma, P. K. *Rev. Sci. Instrum.* **1999**, *70*, 4300.
- (28) Zhuang, X.; Rief, M. *Curr. Opin. Struct. Biol.* **2003**, *13*, 88–97.
- (29) Zinober, R. C.; Brockwell, D. J.; Beddard, G. S.; Blake, A. W.; Olmsted, P. D.; Radford, S. E.; Smith, D. A. *Protein Sci.* **2002**, *11*, 2759–2765.
- (30) Lu, H.; Israilewitz, B.; Krammer, A.; Vogel, V.; Schulten, K. *Biophys. J.* **1998**, *75*, 662.
- (31) Lu, H.; Schulten, K. *Chem. Phys.* **1999**, *247*, 141.
- (32) Schwaiger, I.; Sattler, C.; Hostetter, D. R.; Rief, M. *Nat. Mater.* **2002**, *1*, 232.
- (33) Yang, G.; Cecconi, C.; Baase, W. A.; Vetter, I. R.; Breyer, W. A.; Haack, J. A.; Matthews, B. W.; Dahlquist, F. W.; Bustamante, C. *Proc. Natl. Acad. Sci. U.S.A.* **2000**, *97*, 139.

- (34) Eom, K.; Li, P.-C.; Makarov, D. E.; Rodin, G. J. *J. Phys. Chem. B* **2003**, *107*, 8730.
- (35) Carrion-Vazquez, M.; Li, H.; Lu, H.; Marszalek, P. E.; Oberhauser, A. F.; Fernandez, J. M. *Nat. Struct. Biol.* **2003**, *85*, 2696.
- (36) Li, P.-C.; Makarov, D. E. *J. Chem. Phys.* **2003**, *119*, 9260.
- (37) Heymann, B.; Grubmuller, H. *Chem. Phys. Lett.* **1999**, *303*, 1–9.
- (38) Heymann, B.; Grubmuller, H. *Biophys. J.* **2001**, *81*, 1295–1313.
- (39) Ferrenberg, A. M.; Swendsen, R. H. *Phys. Rev. Lett.* **1989**, *63*, 1195.
- (40) Frenkel, D.; Smit, B. *Understanding Molecular Simulation*, 2nd ed.; Academic Press: San Diego, San Francisco, New York, Boston, London, Sydney, Tokyo, 2002.
- (41) Rohs, R.; Etchebest, C.; Lavery, R. *Biophys. J.* **1999**, *76*, 2760–2768.
- (42) McCammon, J. A.; Harvey, S. C. *Dynamics of proteins and nucleic acids*; Cambridge University Press: Cambridge, 1987.
- (43) Qiu, D.; Shenkin, P. S.; Hollinger, F. P.; Still, W. C. *J. Phys. Chem. A* **1997**, *101*, 3005.
- (44) MacKerell, A. D.; Bashford, D.; Bellott, M.; Dunbrack, R. L.; Evanseck, J. D.; Field, M. J.; Fischer, S.; Gao, J.; Guo, H.; Ha, S.; Joseph-McCarthy, D.; Kuchnir, L.; Kuczera, K.; Lau, F. T. K.; Mattos, C.; Michnick, S.; Ngo, T.; Nguyen, D. T.; Prodhom, B.; Reiher, I. W. E.; Roux, B.; Schlenkrich, M.; Smith, J. C.; Stote, R.; Straub, J.; Watanabe, M.; Wiórkiewicz-Kuczera, J.; Yin, D.; Karplus, M. *J. Phys. Chem. B* **1998**, *102*, 3586.
- (45) Carrion-Vazquez, M.; Oberhauser, A. F.; Fowler, S. B.; Marsalek, P. E.; Broedel, S. E.; Clarke, J.; Fernandez, J. M. *Proc. Natl. Acad. Sci. U.S.A.* **1999**, *96*, 3694–3699.
- (46) Izrailev, S.; Stepaniants, S.; Balsera, M.; Oono, Y.; Schulten, K. *Biophys. J.* **1997**, *72*, 1568–1581.
- (47) Isralewitz, B.; Gao, M.; Schulten, K. *Curr. Opin. Struct. Biol.* **2001**, *11*, 224–230.
- (48) Balsera, M.; Stepaniants, S.; Izrailev, S.; Oono, Y.; Schulten, K. *Biophys. J.* **1997**, *73*, 1281–1287.
- (49) Hanggi, P.; Talkner, P.; Borkovec, M. *Rev. Mod. Phys.* **1990**, *62*, 251.
- (50) Makarov, D. E.; Hansma, P. K.; Metiu, H. *J. Chem. Phys.* **2001**, *114*, 9663.
- (51) Fixman, M.; Kovac, J. *J. Chem. Phys.* **1973**, *58*, 1564.
- (52) Kratky, O.; Porod, G. *Recl. Trav. Chim. Pays-Bas* **1949**, *68*, 1106.
- (53) Marko, J. F.; Siggia, E. *Macromolecules* **1995**, *28*, 209.
- (54) Viani, M. B.; Pietrasanta, L. I.; Thompson, J. B.; Chand, A.; Gebeshuber, I. C.; Kindt, J. H.; Richter, M.; Hansma, H. G.; Hansma, P. K. *Nat. Struct. Biol.* **2000**, *7*, 644.
- (55) Khorasanizadeh, S.; Peters, I. D.; Butt, T. R.; Roder, H. *Biochemistry* **1993**, *32*, 7054–7063.
- (56) Williams, P. M.; Fowler, S. B.; Best, R. B.; Toca-Herrera, J. L.; Scott, K. A.; Steward, A.; Clarke, J. *Nature* **2003**, *422*, 446.
- (57) Truhlar, D. G.; Garrett, B. C.; Klippenstein, S. J. *J. Phys. Chem.* **1996**, *100*, 12771–12800.
- (58) Koradi, R.; Billeter, M.; Wüthrich, K. *J. Mol. Graphics* **1996**, *14*, 51–55.